Minimum Energy Data Transmission for Wireless Networked Control Systems

Yalcin Sadi, *Member, IEEE*, Sinem Coleri Ergen, *Member, IEEE*, and Pangun Park, *Member, IEEE*

***Abstract*—The communication protocol design for wireless networked control systems brings the additional challenge of providing the guaranteed stability of the closed-loop control system compared to traditional wireless sensor networks. In this paper, we provide a framework for the joint optimization of controller and communication systems encompassing efficient abstractions of both systems. The objective of the optimization problem is to minimize the power consumption of the communication system due to the limited lifetime of the battery-operated wireless nodes. The constraints of the problem are the schedulability and maximum transmit power restrictions of the communication system, and the reliability and delay requirements of the control system to guarantee its stability. The formulation comprises communication system parameters including transmission power, rate and scheduling, and control system parameters including sampling period. The resulting problem is a Mixed-Integer Programming problem. However, analyzing the optimality conditions on the variables of the problem allows us to reduce it to an Integer Programming problem for which we propose an efficient solution method based on its relaxation. Simulations demonstrate that the proposed method performs very close to optimal and much better than the traditional separate design of these systems.**

***Index Terms*—Wireless communication, networked control system, optimization, energy minimization, stability.**

I. Introduction

WIRELESS Networked Control Systems (WNCSs) are spatially distributed systems in which sensors, actuators, and controllers connect through a wireless network instead of traditional point-to-point links [1]. WNCSs have a tremendous potential to improve the efficiency of many large-scale distributed systems in industrial automation [2], [3], building automation [4], automated highway [5], air transportation [6], and smart grid [7]. Transmitting sensor measurements and control commands over wireless links provide many benefits such as the ease of installation and maintenance, low complexity and cost, and large flexibility to accommodate the modification and upgrade of the components in many control applications. Several industrial organizations, such as International Society of Automation (ISA) [8], Highway Addressable Remote Transducer (HART) [9], and Wireless Industrial Networking Alliance (WINA) [10], have been actively pushing the application of wireless technologies in the control applications.

Building a WNCS is very challenging since control systems often have stringent requirements on timing and reliability, which are difficult to attain by wireless sensor networks due to the adverse properties of the wireless communication and limited battery resources of the nodes. The wireless communication introduces non-zero packet error probability caused by the unreliability of the wireless transmissions, non-zero delay due to the packet transmission and shared wireless medium, and sampling and quantization errors since the signals are transmitted over the network via packets. Decreasing the packet error probability, delay and sampling period improves the performance of the control system at the cost of more energy consumed in the communication. There is an increasing need for methods and analysis tools that are able to quantify the joint performance of these systems in terms of the communication parameters, including the transmission power, rate and scheduling of the network nodes, the control parameters including the sampling period and wireless communication induced imperfections.

The communication system design for Networked Control Systems (NCS) has received little attention in the literature mainly due to the lack of efficient abstractions of both control and communication systems. The lack of abstractions led to either the simplification of the problem by excluding the key system parameters from the formulation or the solutions through numerical methods avoiding the widespread use of the formulations. Assuming no packet error occurs unless there is a collision in the network, the optimization of the scheduling given the sampling period and delay requirements of the sensors [11], [12] or the optimization of the sampling period and delay parameters of the sensors to minimize the overall performance loss while ensuring the system schedulability [13], [14] have been formulated. These formulations however cannot be applied to WNCS where the packet error probability is non-zero at all times. Some of the prior work on the communication system design for WNCS focus on ensuring low deterministic end-to-end delay and controlled jitter to real-time traffic across a very large mesh network distributed over a large area in a globally synchronized multi-channel Time Division Multiple Access (TDMA) [8], [9], [15], [16]. The optimization problem formulations for WNCS on the other hand aim to determine the best values of the sampling period and network scheduling parameters by using different

Manuscript received July 5, 2013; revised November 1, 2013; accepted January 3, 2014. The associate editor coordinating the review of this paper and approving it for publication was S. Liew.

Y. Sadi and S. C. Ergen are with the Department of Electrical and Electronics Engineering, Koc University, Istanbul, Turkey (e-mail: {ysadi, sergen}@ku.edu.tr). Y. Sadi and S. C. Ergen acknowledge the support of Marie Curie Reintegration Grant IVWSN, PIRG06-GA-2009-256441; The Scientific and Technological Research Council of Turkey Grant #113E233; and Turk Telekom Collaborative Research Award #11315-10.

P. Park is with the Department of Electrical Engineering and Computer Science, University of California Berkeley, Berkeley, CA (e-mail: pgpark@eecs.berkeley.edu). P. Park acknowledges the support of NSF under CPS:ActionWebs (CNS-931843), ONR under the HUNT (N0014-08-0696), SMARTS (N00014-09-1-1051) MURIs and grant N00014-12-1-0609, and AFOSR under the CHASE MURI (FA9550-10-1-0567).

Digital Object Identifier 10.1109/TWC.2014.0204.131204

objective and constraint functions. Some of them aim to minimize the energy consumption of the network subject to the packet loss probability and delay distribution that are derived from the desired control cost [17]. Others aim to maximize the performance of control systems subject to the wireless capacity constraints of the links and the delay requirement of the control system [18]. None of these works however consider the key parameters of the wireless communication system including the transmission power and rate of the links as a system variable to be optimized.

A more general framework where the optimal values of the parameters of the link layer, medium access control layer, and sampling period that minimize the control cost subject to the delay distribution and the packet error probability constraints is proposed in [19]. However, a suboptimal solution is obtained by an iterative numerical method due to the difficulty of dealing with the linear quadratic cost function representing the performance of the control system in the objective of the optimization problem. This numerical approach is hard to be generalized for different requirements of various control applications.

Joint optimization of the transmission power control, rate adaptation, and scheduling has been widely studied for delay constrained energy minimization in general purpose wireless networks [20]–[27]. Different algorithms have been proposed for the solution of the optimization problem depending on the delay constraint in terms of either a single deadline to all packets [20]–[23] or individual deadlines for each packet [24]–[26] and the usage of either a fixed capacity battery [20], [21], [24], [25], [26] or a finite storage capacity rechargeable battery [22], [23]. None of these algorithms however have been extended to formulate the joint optimization of power, rate and scheduling for energy minimization while meeting a certain controller performance.

The goal of this paper is to study the joint optimization of controller and communication systems taking into account all the wireless network induced imperfections including packet error and delay; the parameters of the wireless communication system including the transmission power, rate and scheduling of the network nodes; and the parameters of the controller including the sampling period. The objective of the optimization problem is to minimize the power consumption of the communication system whereas the constraints guarantee the stability of the control system and the schedulability in the communication system. The original contributions of this paper are listed as follows:

- We provide a framework for the joint optimization of controller and communication systems encompassing efficient abstractions of both systems, which may lead to broader adoption and real-world deployment.
- We formulate the joint optimization of controller and communication systems for MQAM modulation in a network containing multiple sensors communicating with their corresponding controllers as a Mixed Integer Programming problem.
- We propose an efficient solution method for the formulated optimization problem based on the analysis of the relations between the optimal values of the decision variables.

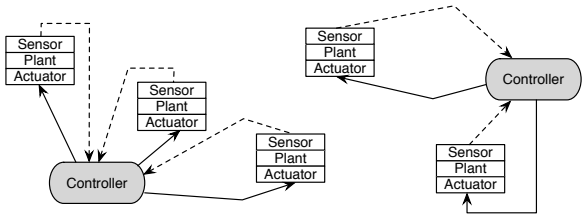

Fig. 1. Overview of the WNCS setup.

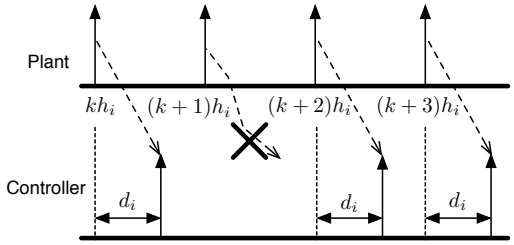

Fig. 2. Timing diagram between a plant and a controller communicating over a wireless network.

- We prove the energy saving of the proposed joint optimization problem over the traditional separate design of controller and communication systems and the closeness to the optimality of the proposed solution method via extensive simulations.

The rest of the paper is organized as follows. Section II describes the system model and the assumptions used throughout the paper. Section III presents the control and communication system models. The joint optimization of controller and communication systems has been formulated in Section IV. Simulations are presented in Section V. Finally concluding remarks are given in Section VI.

II. System Model and Assumptions

The system model and assumptions are detailed as follows.

1) Fig. 1 depicts the architecture of a WNCS where multiple plants are controlled over a wireless network. We assume that a sensor node is attached to each plant. Outputs of the plants are sampled at periodic intervals by the sensors and forwarded to the controller over a wireless network, which induces delays and packet errors. When the controller receives the measurements, a new control command is computed. The control command is forwarded to the actuator attached to the plant. We assume that the controller commands are successfully received by the actuator. Many practical NCSs have several sensing channels, whereas the controllers are collocated with the actuators, as in heat, ventilation and air conditioning control systems, because the control command is very critical [28]. One of the controllers is assigned as the network manager.
2) Fig. 2 illustrates various possible situations of the information exchange between a plant and a controller. Let us denote the sampling period of node i by h_i, the transmission delay of the packet that includes the sample of the sensor node by d_i, and the packet error probability

by p_i. We assume that $d_i \leq h_i$ to guarantee that the packets arrive to the controller in the correct order. The retransmission of outdated packets are generally not useful since the latest information of the plant state is the most critical information for control applications [1]. We also assume that the packet error is modeled as a Bernoulli random process with probability p_i for node i to simplify the problem.

3) We consider TDMA as MAC protocol since TDMA provides both delay guarantee and energy efficiency to the networks with predetermined topology and data generation patterns [29] thus is widely used in industrial control applications [8], [9]. The details of synchronization and topology discovery mechanisms for energy efficient TDMA are out of scope of this paper and can be found in [29].
4) The time is partitioned into frames. Each frame is further divided into a beacon and time slots. The beacon is used by the network manager to provide time synchronization within the WNCS and broadcast updates on the scheduling decisions. The scheduling decisions include the time slot allocation and the values of the optimal node parameters including the transmission power, rate and sampling period corresponding to each sensor node. We assume that no concurrent transmissions are scheduled. The network manager continually monitors the received power and the packet error rate over each link. If the channel conditions do not change, the beacon only provides synchronization information. Otherwise, the beacon also includes the updates on the scheduling decisions. Despite the updates on the schedule and optimal node parameters, the length of the frame is fixed as derived mathematically in Section IV.
5) The nodes are assumed to operate their radio in sleep mode when they are not scheduled to transmit or receive a packet, and transient mode when they switch from sleep mode to active mode to transmit or receive a packet and vice versa. We consider only the energy consumption in the transmission of the packets in the optimization problem because it is much larger than that in the sleep and transient modes [20], [27] and the energy consumption in the reception of the beacon packets is fixed.

III. Control and Communication System Models

This section provides control and communication system models based on the consideration of the stability of the control system, the restrictions related to the wireless communication and the power consumption of the communication system.

A. Control System Model

The performance and stability conditions for the control systems have been formulated in the form of Maximum Allowable Transfer Interval (MATI), defined as the maximum allowed time interval between subsequent state vector reports from the sensor nodes to the controller, and Maximum Allowable Delay (MAD), defined as the maximum allowed packet delay for the transmission from the sensor node to the controller, in [30], [31], [32], [33]. Such hard real-time guarantees can be satisfied by wireline networks but is an unreasonable expectation for wireless networks where the packet error probability is greater than zero at any point in time. Hence, many control applications such as wireless industrial automation [8], air transportation systems [6] and autonomous vehicular systems [34] set a stochastic MATI constraint in the form of keeping the time interval between subsequent state vector reports above the MATI value with a predefined probability to guarantee the stability of control systems. Stochastic MATI and MAD constraints are efficient abstractions of the performance of the control systems however have not been considered before in the joint design with the communication systems.

1) Stochastic MATI Constraint: Stochastic MATI constraint is formulated as

$$\Pr\left[\mu_i(h_i, d_i, p_i) \leq \Omega\right] \geq \delta \tag{1}$$

where μ_i is the time interval between subsequent state vector reports of node i as a function of h_i, p_i and d_i; Ω is the MATI; and δ is the minimum probability with which MATI should be achieved. The values of Ω and δ are determined by the control system.

In order that the time interval between subsequent state vector reports of node i is less than Ω, there should be at least one successful transmission within Ω. Given h_i and Ω, the number of reception opportunities of the state vector reports is $\left\lfloor \frac{\Omega}{h_i} \right\rfloor$. Based on the assumption that the packet error is modeled as a Bernoulli random process with probability p_i for node i, stochastic MATI constraint given in Eq. (1) can be rewritten as

$$1 - p_i^{\left\lfloor \frac{\Omega}{h_i} \right\rfloor} \geq \delta\,. \tag{2}$$

Many control applications and standards define the stochastic MATI requirements to guarantee the stability of the control systems. In industrial automation, closed-loop machine controls have specified $\Omega = 100$ ms and $\delta = 0.999$ [8], [35]. Moreover, to allow IEEE 802.15.4 devices [36] to support a wide range of industrial applications, IEEE 802.15.4e standard [37] specifies an amendment to the IEEE 802.15.4 standard to enhance its latency and reliability performances for industrial automation. They have specified $\Omega = 10$ ms and $\delta = 0.99$. In addition, the air transportation system requires $\Omega = 4.8$ s and $\delta = 0.95$ [6]. Furthermore, the requirements of cooperative vehicular safety applications are given by $\Omega = 100$ ms and $\delta = 0.95$ [34].

2) MAD Constraint: MAD constraint should be included in addition to the MATI constraint to guarantee the performance and stability of the control systems [33]. MAD constraint is formulated as

$$d_i \leq \Delta \tag{3}$$

where Δ is the MAD to stabilize the control system. The value of Δ is determined by the control system and typically on the order of a few tens of milliseconds for fast control applications [8], [35], [38].

B. Communication System Model

This section provides the formulations of the power consumption of the sensor nodes, the maximum transmit power and schedulability constraints of the communication system. The power consumption of the sensor node is formulated as a function of its sampling period, delay and packet error probability for both uncoded and trellis-coded MQAM modulation. The reason for choosing a specific modulation and coding strategy instead of the information theoretically optimal channel coding schemes is to include the trade-off between the packet error probability and power consumption in practical communication systems. The optimal channel coding schemes do not allow including such trade-off since they employ randomly generated codes with exponentially small probability of error for long block lengths [39]. Moreover, choosing a specific modulation strategy allows us to include the circuit power in addition to the transmission power consumption [27]. The proposed formulation for MQAM modulation can be extended for any modulation strategy.

1) Power Consumption: The key design concern of the communication protocol is to limit the energy consumed by the sensor devices. This will avoid battery replacement resulting in an affordable WNCS deployment.

The power consumption of the node i as a function of its sampling period, delay and packet error probability is formulated as

$$W_i\left(h_i, d_i(b_i), p_i\right) = \frac{\left(W_i^t\left(d_i(b_i), p_i\right) + W_i^c\right) d_i(b_i)}{h_i} \tag{4}$$

where b_i is the number of bits used per symbol and d_i is represented as a function of b_i for a given modulation scheme, W_i^t is the transmission power calculated as a function of the parameters d_i and p_i for a given modulation and channel coding, and W_i^c is the circuit power consumption in the active mode at the transmitter. The numerator provides the energy consumed for the transmission of duration $d_i(b_i)$ in one sampling period h_i. In the following, we present the formulation of $W_i^t(d_i(b_i), p_i)$ for MQAM modulation scheme based on the assumption of an additive white Gaussian noise (AWGN) channel by summarizing the derivation procedure in [27] for completeness.

Let us denote the number of bits sent by node i by L_i. $b_i = \log_2 M$ is the number of bits per symbol for MQAM and $b_i = 2$ is the minimum allowable value ensuring MQAM is well defined [27]. The number of MQAM symbols needed to send L_i bits is equal to both L_i/b_i and d_i/T^s, where T^s is the symbol period. If square pulses are used and $T^s \approx 1/B$, where B is the bandwidth, then

$$d_i(b_i) \approx \frac{L_i}{B b_i}\,. \tag{5}$$

A bound on the probability of bit error for MQAM is given by [40]

$$P_i^b \leq \frac{4}{b_i}\left(1 - \frac{1}{\sqrt{2^{b_i}}}\right) e^{-\frac{3}{2^{b_i}-1}\frac{\gamma_i}{2}} \tag{6}$$

where P_i^b is the probability of bit error of node i, γ_i is the Signal-to-Noise Ratio (SNR) of node i defined as $\gamma_i = \frac{W_i^r}{2B\sigma^2 N^f}$, where W_i^r is the signal power received from node i, σ^2 is the power spectral density of the AWGN and N^f is the noise figure. By approximating this bound as an equality and using the relation between the transmission power and received power as $W_i^t = W_i^r G_i$ where G_i is the power gain factor, and the function mapping b_i to d_i in Eq. (5), the transmission power as a function of b_i and P_i^b is given by

$$W_i^t(b_i, p_i) \approx \frac{4}{3} N^f \sigma^2 B G_i \left(2^{b_i} - 1\right) \ln \frac{4\left(1 - 2^{-\frac{b_i}{2}}\right)}{b_i P_i^b}\,. \tag{7}$$

If no error control mechanism is used, a packet is considered to be in error in the presence of one or more bit errors. Assuming independent bit errors, the packet error probability p_i is given by

$$p_i = 1 - \left(1 - P_i^b\right)^{L_i} \approx P_i^b L_i \tag{8}$$

for small values of P_i^b where the approximation is obtained by finding the Taylor series expansion of $\left(1 - P_i^b\right)^{L_i}$ and ignoring higher order terms.

If forward error correction codes are used, the required value of SNR to meet a target bit error probability decreases by a factor called coding gain denoted by G^c at the cost of resulting bandwidth expansion in order to communicate the extra redundant bits. Fortunately, bandwidth expansion can be circumvented when the channel coding and modulation processes are jointly designed, for instance, in trellis-coded MQAM [40]. The decrease in the required SNR results in the decrease in the required transmission power W_i^t for the same bit error probability.

By substituting Eqs. (7) and (8) into Eq. (4), the power consumption for trellis-coded MQAM is formulated as

$$W_i(h_i, b_i, p_i) = \frac{4N^f \sigma^2 G_i L_i}{3G^c h_i b_i}\left(2^{b_i} - 1\right) \ln \frac{4L_i\left(1 - 2^{-\frac{b_i}{2}}\right)}{p_i b_i} + \frac{W_i^c L_i}{B h_i b_i}.$$

2) Maximum Transmit Power Constraint: We assume that there exists a maximum power level, denoted by $W^{t,\max}$, that a node can use for transmission. This is enforced by the limited weight and size of the sensor nodes. The maximum transmit power constraint is formulated as

$$W_i^t(b_i, p_i) \leq W^{t,\max} \tag{9}$$

where

$$W_i^t(b_i, p_i) = \frac{4N^f \sigma^2 G_i B}{3G^c}\left(2^{b_i} - 1\right) \ln \frac{4L_i\left(1 - 2^{-\frac{b_i}{2}}\right)}{p_i b_i}\,. \tag{10}$$

3) Schedulability Constraint: The schedulability constraint represents the allocation of the transmission times of multiple sensor nodes in the network in the absence of concurrent transmissions using pre-emptive Earliest Deadline First (EDF) scheduling algorithm. EDF is a dynamic scheduling algorithm where the task closest to its deadline is scheduled whenever a scheduling event occurs. EDF has been proven to be an optimal uniprocessor scheduling algorithm for periodic tasks with certain deadlines using pre-emption, in the following sense: If a real-time task set cannot be scheduled by EDF, then this task set cannot be scheduled by any algorithm [41]. For the case where there exists a node such that its deadline is not equal to its period, i.e. $\exists i \in [1, N], \Delta \neq h_i$, there exists an exact schedulability analysis based on the simulation of the

EDF algorithm for a time duration formulated as a function of d_i, h_i, Δ and task arrival times a_i for all $i \in [1, N]$: The EDF schedule is generated for the specified time duration and given values of d_i, h_i, Δ and a_i for all $i \in [1, N]$ are declared feasible if and only if no deadlines are missed in this schedule [42], [43]. This simulation based schedulability analysis however cannot be used in an optimization framework where the explicit formulations of the necessary and sufficient conditions for the schedulability are required. Since such explicit formulations do not exist, we propose the use of the schedulability constraint given by

$$\sum_{i=1}^{N} \frac{d_i}{h_i} \leq \beta \tag{11}$$

where β is the utilization bound satisfying $0 < \beta \leq 1$ in our optimization framework. The use of this new schedulability constraint is demonstrated to provide near-optimal solutions via simulations in Section V when the value of β is adapted to the network topology and requirements as described in the following.

Lemma 1: For $\beta = \beta_{nec} = 1$, the schedulability constraint given by Eq. (11) is a necessary condition for a feasible schedule.

Proof: Every term $\frac{d_i}{h_i}$ in Eq. (11) represents the ratio of the total time duration allocated for the transmission of node i to the schedule length. Since there are no concurrent transmissions, the sum of these terms gives the ratio of the total time duration allocated to all the nodes $i \in [1, N]$ to the schedule length. The value of this ratio cannot exceed 1 since the sum of the time durations allocated to all the nodes in a schedule cannot exceed the schedule length. □

Lemma 2: For $\beta = \beta_{suf} = \min\{1, \min_{i\in[1,N]} \frac{\Delta}{h_i}\}$, the schedulability constraint given by Eq. (11) is a sufficient condition for a feasible schedule.

Proof: For the specified value of $\beta = \beta_{suf}$, Eq. (11) can be reformulated as

$$\sum_{i=1}^{N} \frac{d_i}{h_i \min\{1, \min_{i\in[1,N]} \frac{\Delta}{h_i}\}} \leq 1 \tag{12}$$

Since

$$\sum_{i=1}^{N} \frac{d_i}{\min\{\Delta, h_i\}} \leq 1 \tag{13}$$

is a sufficient condition for a feasible schedule [44], and

$$\sum_{i=1}^{N} \frac{d_i}{h_i \min\{1, \min_{i\in[1,N]} \frac{\Delta}{h_i}\}} \geq \sum_{i=1}^{N} \frac{d_i}{\min\{\Delta, h_i\}} \tag{14}$$

Eq. (11) is also a sufficient condition for $\beta = \beta_{suf}$. □

β_{nec} and β_{suf} in Lemmas 1 and 2 provide the upper and lower values of the utilization bound respectively. Using a β value larger than β_{nec} expands the feasible region of the corresponding optimization problem by infeasible schedules whereas using a β value smaller than β_{suf} shrinks the feasible region by removing the schedules satisfying $\beta < \sum_{i=1}^{N} \frac{d_i}{h_i} \leq \beta_{suf}$ from the feasible region of the corresponding optimization problem. Moreover, increasing the value of β expands the feasible region of the optimization problem. Therefore, the maximum value of $\beta \in [\beta_{suf}, \beta_{nec}]$ that yields a feasible schedule for an optimization problem needs to be determined as explained in detail in Section IV-B.

IV. Joint Optimization of Control and Communication Systems

This section formulates the problem of the joint optimization of control and communication systems with the objective of minimizing the power consumption of the network subject to the stochastic MATI and MAD constraints guaranteeing the stability of the control systems and maximum transmit power and schedulability constraints of the wireless communication system. The key in formulating this optimization problem is the trade-off between the control performance and the power consumption of the wireless communication network. Decreasing the packet error probability, delay and sampling period improves the performance of the control system at the cost of more energy consumed in the communication. The sampling period, packet error probability, and delay must therefore be flexible design parameters that need to be adequate for the control requirements.

The joint optimization of control and communication systems is formulated as

$$\min_{h_i, b_i, p_i, i\in[1,N]} \quad \sum_{i=1}^{N} W_i(h_i, b_i, p_i) \tag{15a}$$

$$\text{s.t.} \quad \sum_{i=1}^{N} \frac{d_i(b_i)}{h_i} \leq \beta\,, \tag{15b}$$

$$1 - p_i^{\left\lfloor \frac{\Omega}{h_i} \right\rfloor} \geq \delta, \quad \forall i \in [1, N]\,, \tag{15c}$$

$$0 < d_i(b_i) \leq \min\{\Delta, h_i\}, \tag{15d}$$

$$0 < h_i \leq \Omega, \tag{15e}$$

$$0 < p_i < 1, \tag{15f}$$

$$W_i^t(b_i, p_i) \leq W^{t,\max}, \tag{15g}$$

where N is the number of nodes in the network.

The goal of the optimization problem is to minimize the total power consumption in the network. Eq. (15b) represents the schedulability constraint. Eqs. (15c) and (15d) represent the stochastic MATI and MAD constraints respectively. Eq. (15e) states that the sampling period of the nodes must be less than or equal to the MATI. Eq. (15f) states the lower and upper bounds for the packet error probability. Finally, Eq. (15g) represents the maximum transmit power constraint. The variables of the problem are $h_i, i \in [1, N]$, the sampling period of the nodes; $b_i, i \in [1, N]$, the number of bits used per symbol for each node; and $p_i, i \in [1, N]$, the packet error probability of the nodes.

This optimization problem is non-convex Mixed-Integer Programming problem thus difficult to solve for the global optimum [45]. We now analyze the optimality conditions for this problem and propose efficient solution methods for the network containing one sensor node, i.e. N=1, and multiple sensor nodes in Sections IV-A and IV-B respectively.

A. One Sensor Case

The joint optimization of control and communication systems for the network containing one sensor node is formulated as

$$\min_{h_i,b_i,q_i} \quad C_{i1}\frac{2^{b_i}-1}{h_i b_i}\left(\ln\frac{4L_i\left(1-2^{\frac{-b_i}{2}}\right)}{b_i}-q_i\right)+\frac{W_i^c C_{i2}}{h_i b_i} \tag{16a}$$

$$\text{s.t.} \quad \left\lfloor\frac{\Omega}{h_i}\right\rfloor q_i-\ln(1-\delta)\le 0, \tag{16b}$$

$$0<d_i(b_i)\le\min\{\Delta,h_i\}, \tag{16c}$$

$$0<h_i\le\Omega, \tag{16d}$$

$$q_i\le 0, \tag{16e}$$

$$\frac{C_{i1}}{C_{i2}}\left(2^{b_i}-1\right)\left(\ln\frac{4L_i\left(1-2^{-\frac{b_i}{2}}\right)}{b_i}-q_i\right)\le W^{t,\max}. \tag{16f}$$

where $C_{i1}=\frac{4N^f\sigma^2G_iL_i}{3G^c}$ and $C_{i2}=\frac{L_i}{B}$. The new variable q_i is equal to $\ln p_i$. The objective function in Equation (16a) includes the power consumption formulation defined in Equation (15a) for $N=1$ and MQAM. The constraint given in Eq. (15b) is eliminated since the constraint in Eq. (15d) is already sufficient for schedulability when $N=1$. The constraints in Eqs. (16b), (16c), (16d), (16e) and (16f) correspond to the constraints given in Eqs. (15c), (15d), (15e), (15f) and (15g) respectively for $N=1$ and MQAM.

The optimization problem is again a non-convex Mixed-Integer Programming problem thus difficult to solve for the global optimum [45]. Next, we will investigate the relations between the optimal values of h_i and q_i, denoted by h_i^* and q_i^* respectively, to that of b_i, denoted by b_i^*, so that we can rewrite this problem as an Integer Programming (IP) problem, including only b_i as a variable and eliminating h_i and q_i, for which there are efficient approximation algorithms [45].

Lemma 3: The optimal value of the sampling period is given by

$$\frac{\Omega}{h_i^*}=k_i \tag{17}$$

where k_i is a positive integer.

Proof: We prove the Lemma by contradiction. Suppose that $\frac{\Omega}{h_i^*}$ is not a positive integer then $\left\lfloor\frac{\Omega}{h_i^*}\right\rfloor<\frac{\Omega}{h_i^*}$. If h_i^* increases such that the equality $\left\lfloor\frac{\Omega}{h_i^*}\right\rfloor=\frac{\Omega}{h_i^*}$ holds for the first time while satisfying the upper bound given in Eq. (16d), the stochastic MATI constraint given in Eq. (16b) still holds since the value of $\left\lfloor\frac{\Omega}{h_i^*}\right\rfloor$ does not change. The remaining constraint including h_i given in Eq. (16c) also still holds with this change. However, the power consumption given in Eq. (16a) decreases since it is a monotonically decreasing function of h_i. □

Lemma 4: In the optimal solution, the stochastic MATI is satisfied with equality such that

$$\frac{\Omega}{h_i^*}=\frac{\ln(1-\delta)}{q_i^*}=k_i \tag{18}$$

where k_i is a positive integer.

Proof: We prove the Lemma by contradiction. Suppose that

$$\frac{\Omega}{h_{i^*}}>\frac{\ln(1-\delta)}{q_i^*} \tag{19}$$

If q_i^* increases such that the stochastic MATI constraint is satisfied with equality, the constraints given in Eqs. (16e) and (16f) still hold. However, the power consumption given in Eq. (16a) decreases since it is a monotonically decreasing function of q_i. Then the result follows when combined with Lemma 3. □

Next, we eliminate the variables h_i and q_i from the optimization problem (16) by using the expressions derived in Lemma 4 for their optimal values as a function of the single variable k_i. Note that k_i is the number of transmissions within Ω. The joint optimization of control and communication systems is then reformulated as

$$\min_{b_i,k_i} \quad C_{i1}\frac{(2^{b_i}-1)k_i}{\Omega b_i}\left(\ln\frac{4L_i(1-2^{\frac{-b_i}{2}})}{b_i}-\frac{\ln(1-\delta)}{k_i}\right)+\frac{W^cC_{i2}k_i}{\Omega b_i} \tag{20a}$$

$$\text{s.t.} \quad 0<d_i(b_i)\le\min\left\{\Delta,\frac{\Omega}{k_i}\right\}, \tag{20b}$$

$$\frac{C_{i1}}{C_{i2}}\left(2^{b_i}-1\right)\left(\ln\frac{4L_i\left(1-2^{-\frac{b_i}{2}}\right)}{b_i}-\frac{\ln(1-\delta)}{k_i}\right)\le W^{t,\max}, \tag{20c}$$

where the constraints given in Eqs. (20b) and (20c) correspond to those in Eqs. (16c) and (16f) respectively and the remaining constraints in the optimization problem (16) are removed due to the additional constraint of k_i being a positive integer. The following lemma expresses the optimal value of k_i in terms of b_i so that the above optimization problem can be formulated with the variable b_i only.

Lemma 5: Based on the assumption that the optimization problem (20) is feasible, the optimal value of k_i denoted by k_i^* is expressed as a function of b_i as

$$k_i^*=k_i(b_i)=\max\left\{1,\left\lceil\frac{\ln(1-\delta)}{\ln\frac{4L_i(1-2^{-\frac{b_i}{2}})}{b_i}-\frac{W^{t,\max}C_{i2}}{G^cC_{i1}(2^{b_i}-1)}}\right\rceil\right\} \tag{21}$$

Proof: Since the power consumption given by Eq. (20a) is a monotonically increasing function of k_i, k_i^* is the minimum positive integer satisfying Eqs. (20b) and (20c). The second term of the maximum in Eq. (21) is the minimum k_i value satisfying Eq. (20c) since Eq. (20b) is satisfied by this minimum k_i value if there exists a feasible solution. □

Note that k_i is a non-decreasing function of b_i. Let us call $b_i^{\min}$ and $b_i^{\max}$ the minimum and maximum value of b_i satisfying the constraints given in Eqs. (20b) and (20c). In the following, Lemma 6 and Theorem 1 derive the relation between the optimal value of k_i and these boundary values $b_i^{\min}$ and $b_i^{\max}$.

Lemma 6: For two feasible consecutive constellation size

values b_i and b_i+1, if $k_i(b_i) \geq 2$, then $k_i(b_i+1) \geq \frac{3}{2}k_i(b_i)$.

Proof: If $k_i(b_i) \geq 2$ then the second term in the maximum operator in Eq. (21) is effective such that

$$k_i(b_i) = \left\lceil \frac{\ln(1-\delta)}{\ln \frac{4L_i(1-2^{-\frac{b_i}{2}})}{b_i} - \frac{W^{t,\max}C_{i2}}{G^c C_{i1}(2^{b_i}-1)}} \right\rceil \tag{22}$$

Since $k_i(b_i) \geq 2$, the denominator of the above expression is negative. If b_i increases by 1, the first term in the denominator decreases by a factor of at most 2 whereas the second term in the denominator decreases by a factor of at least 2 resulting in a factor of at least 2 decrease in the denominator such that

$$\frac{\ln \frac{4L_i(1-2^{-\frac{b_i}{2}})}{b_i} - \frac{W^{t,\max}C_{i2}}{G^c C_{i1}(2^{b_i}-1)}}{\ln \frac{4L_i(1-2^{-\frac{b_i+1}{2}})}{b_i+1} - \frac{W^{t,\max}C_{i2}}{G^c C_{i1}(2^{b_i+1}-1)}} \geq 2 \tag{23}$$

Due to the ceiling operation in the expression of $k_i(b_i)$, a factor of at least 2 decrease in the denominator results in a factor of at least $\frac{3}{2}$ increase in $k_i(b_i)$ for $k_i(b_i) \geq 2$. □

***Theorem** 1:* The optimal value of $k_i(b_i)$ is given by

$$k_i^*(b_i) = k_i(b_i^{\min}) \tag{24}$$

Proof: We prove the Theorem by contradiction. Suppose that $k_i^*(b_i)$ is not equal to $k_i(b_i^{\min})$ such that $k_i^*(b_i) \geq 2$. Decreasing b_i by one decreases the power consumed in the actual data transmission; i.e., first term of Eq. (20a), since it is an increasing function of both b_i and k_i. Decreasing b_i by one also decreases the circuit power consumption; i.e., second term of Eq. (20a), since it is an increasing function of b_i for $b_i \geq 2$ based on Lemma 6 that states that $k_i(b_i-1) \leq \frac{2k_i^*(b_i)}{3}$ if $k_i(b_i-1) \geq 2$ and the fact that $k_i(b_i-1) \leq \frac{2k_i^*(b_i)}{3}$ if $k_i(b_i-1) = 1$ and $k_i^*(b_i) \geq 2$. The power consumption can therefore further decrease if we decrease b_i by one. This is a contradiction. □

The joint optimization of control and communication systems is then reformulated as

$$\min_{b_i} \quad C_{i1}\frac{(2^{b_i}-1)k_i(b_i^{\min})}{\Omega b_i}\left(\ln \frac{4L_i(1-2^{\frac{-b_i}{2}})}{b_i} - \frac{\ln(1-\delta)}{k_i(b_i^{\min})}\right) + \frac{W_i^c C_{i2}k_i(b_i^{\min})}{\Omega b_i} \tag{25a}$$

$$\text{s.t.} \quad b_i^{\min} \leq b_i \leq b_i^{\max}, \tag{25b}$$

where $b_i^{\min}$ is determined by using Eq. (20b) and $b_i^{\max}$ is the maximum value of b_i such that the corresponding $k_i(b_i)$ value determined by using Eq. (21) is equal to $k_i(b_i^{\min})$.

This optimization problem is an IP problem for which there is no known polynomial-time algorithm [46]. We therefore propose the following heuristic algorithm. We first use the upper bound

$$\ln \frac{4L_i(1-2^{\frac{-b_i}{2}})}{b_i} \leq \ln \frac{4L_i(1-2^{\frac{-b_i^{\min}}{2}})}{b_i^{\min}}. \tag{26}$$

in the objective function (25a). The relaxation of the problem (25) in which the integrality constraint on the constellation size b_i is removed is then a convex optimization problem and can be solved optimally by using interior point method [45]. However, the solution of the relaxed problem is generally not integer. Since the constellation size must be integer, the optimal solution is one of the two neighboring integer values of the solution of the relaxed problem. The best integer solution can be determined by evaluating the power consumption corresponding to these two integer values and choosing the one with the minimum power.

In the following, we summarize the entire procedure for solving the joint optimization of control and communication systems for the network containing one sensor node:

1) Determine $b_i^{\min}$ and $k_i^*(b_i) = k_i(b_i^{\min})$: We determine the minimum b_i value based on Eq. (20b), which requires satisfying both $0 < d_i(b_i) \leq \Delta$ and $0 < d_i(b_i) \leq \frac{\Omega}{k_i(b_i)}$ constraints. We first determine the minimum b_i value satisfying $0 < d_i(b_i) \leq \Delta$. Then, $k_i(b_i)$ value is determined based on Eq. (21). If $0 < d_i(b_i) \leq \frac{\Omega}{k_i(b_i)}$ is also satisfied using these values of b_i and $k_i(b_i)$ then minimum feasible constellation size $b_i^{\min}$ is equal to that particular b_i. Otherwise, b_i is incremented by 1 until $0 < d_i(b_i) \leq \frac{\Omega}{k_i(b_i)}$ constraint is satisfied. Once $b_i^{\min}$ is determined, $k_i^*(b_i) = k_i(b_i^{\min})$.
2) Determine $b_i^{\max}$: Given the optimal value $k_i^*(b_i)$, $b_i^{\max}$ is the maximum value of b_i such that $k_i(b_i) = k_i(b_i^{\min})$ considering Eq. (21).
3) Determine h_i^* and q_i^*: Given the optimal value $k_i^*(b_i)$, the optimal h_i^* and q_i^* values are determined based on Eq. (18).
4) Determine b_i^*: Solve the relaxation of the optimization problem (25) using the bound given by Eq. (26) and determine the best integral solution as b_i^*.

The only suboptimality of this procedure comes from the use of the bound given by Eq. (26). The use of this bound results in an error less than 5% in the total power consumption when b_i is within the range $[2, 20]$ (which is a reasonable range for practical MQAM systems) and the other parameters are set as given in Table I. However, the effect of this error on the optimal total power consumption is much less than 5% in most scenarios as illustrated through simulations in Section V.

B. Multiple Sensor Case

The joint optimization of control and communication systems for the network containing multiple sensor nodes only brings the additional schedulability constraint given by Eq. (15b). The schedulability constraint is the only constraint requiring a joint decision for multiple sensor nodes since the remaining constraints represent the individual constraints of the nodes already considered in Section IV-A.

The findings derived in Lemmas 3-6 for the network containing one sensor node still hold in the existence of the schedulability constraint of multiple sensor nodes since they are not related to the schedulability constraint. The schedulability constraint of multiple sensor nodes can therefore be rewritten as

$$\sum_{i=1}^{N} \frac{C_{i2}k_i(b_i)}{\Omega b_i} \leq \beta \tag{27}$$

This schedulability constraint can be simplified based on the following Lemma.

Lemma 7: The optimal value of $k_i(b_i)$ in the schedulability constraint given by Eq. (27) is equal to $k_i(b_i^{min})$ for each node $i \in [1, N]$.

Proof: Using minimum $k_i(b_i)$ value for every $i \in [1, N]$ minimizes each term $\frac{C_{i2}k_i(b_i)}{\Omega b_i}$ in the schedulability constraint and each power consumption term in the objective function of the joint optimization problem (15) based on Theorem 1. Therefore, the sum of these terms are also minimized with $k_i(b_i^{min})$ for every $i \in [1, N]$.□

The schedulability constraint can therefore be reformulated as

$$\sum_{i=1}^{N} \frac{C_{i2}k_i(b_i^{min})}{\Omega b_i} \leq \beta \tag{28}$$

The optimal solution procedure derived for one sensor case can be extended to the multiple sensor case by determining first $b_i^{\min}$, $k_i^*(b_i) = k_i(b_i^{\min})$, $b_i^{\max}$, h_i^* and q_i^* separately for each sensor $i \in [1, N]$ then b_i^* for $i \in [1, N]$ via solving the joint optimization problem formulated as

$$\min_{b_i, i\in[1,N]} \quad \sum_{i=1}^{N} \frac{C_{i1}(2^{b_i}-1)k_i^{\min}}{\Omega b_i} \left(\ln \frac{4L_i(1-2^{\frac{-b_i}{2}})}{b_i} - \frac{\ln(1-\delta)}{k_i^{\min}} \right) + \frac{W_i^c C_{i2} k_i^{\min}}{\Omega b_i} \tag{29a}$$

$$\text{s.t.} \quad \sum_{i=1}^{N} \frac{C_{i2}k_i(b_i^{\min})}{\Omega b_i} \leq \beta\,, \tag{29b}$$

$$b_i^{\min} \leq b_i \leq b_i^{\max}\,, \quad \forall i \in [1, N]. \tag{29c}$$

This optimization problem is an IP problem for which there is no known polynomial-time algorithm [46]. Similar to the one sensor case, the following heuristic algorithm is proposed to solve this problem. We first use the bound given in Eq. (26). The relaxation of this problem in which the integrality constraint on the constellation sizes is removed is again a convex optimization problem thus can be solved optimally by using interior point method [45]. The resulting optimal values of the constellation sizes are possibly non-integer therefore ceiled to obtain an integral solution while avoiding the violation of the schedulability constraint.

Based on the above observations, the length of the scheduling frame defined in Section II can be chosen to be equal to $n_{MATI}\Omega$ where n_{MATI} is a positive integer fixed over time. Since the optimal period h_i^* of each node $i \in [1, N]$ is given by $\frac{\Omega}{k_i^*}$ for some positive integer k_i^* due to Lemmas 3 and 5, the scheduling of the nodes repeats every time duration of length Ω if the channel conditions do not change. An integer multiple of the time duration Ω is therefore suitable to update the schedule. Since a beacon is transmitted at the beginning of each frame, the value of n_{MATI} is chosen depending on the synchronization accuracy required by the system and the speed at which the channel conditions change.

As explained in Section III-B3, we need to determine the maximum value of the utilization bound $\beta \in [\beta_{suf}, \beta_{nec}]$ for which the solution of the joint optimization problem (29) yields a feasible EDF schedule, which is denoted by β_{opt}. The overall procedure of generating the feasible EDF schedule corresponding to β_{opt} given in Algorithm 1 is described next. The upper and lower bounds of β_{opt}, denoted by β_{up} and β_{low} respectively, are initialized to $\beta_{nec} = 1$ and $\beta_{suf} = \min\{1, \min_{i\in[1,N]} \frac{\Delta}{h_i^*}\}$ based on Lemmas 1 and 2 respectively (Lines 1-2). The joint optimization problem (29) with the value of β initialized to β_{up} (Line 3) is solved for the optimal delay values d_i^* for all $i \in [1, N]$ (Line 4, **solveOptim**(β) function returns the optimal delay values d_i^* corresponding to the optimal constellation size values b_i^* for all $i \in [1, N]$ obtained via solving the optimization problem (29) with a particular value of β). The existence of a feasible schedule using these optimal delay values and the optimal period values obtained by the procedure described in Section IV-A is then checked by performing the exact schedulability analysis of the EDF scheduling algorithm (Line 5, **isSchedulable**($\{h_i, d_i, i \in [1, N]\}$) function returns true if there exists a feasible schedule corresponding to the given period and delay values and false otherwise. The exact schedulability analysis is based on the simulation of the EDF algorithm for the time duration τ formulated as

$$\tau = \frac{c}{1-c} \max_{i\in[1,N]} \{h_i - \Delta\} \tag{30}$$

where $c = \sum_{i=1}^{N} \frac{d_i}{h_i}$ [42]. However, since the scheduling of the nodes repeats every time duration of length Ω given that the optimal period $h_i^* = \frac{\Omega}{k_i^*}$ for some positive integer k_i^* for all $i \in [1, N]$ due to Lemmas 3 and 5, it is enough to perform the schedulability analysis over the time duration of $\min\{\tau, \Omega\}$. **isSchedulable**($\{h_i, d_i, i \in [1, N]\}$) simply generates the EDF schedule for the time duration equal to $\min\{\tau, \Omega\}$ and declares that there exists a feasible schedule if and only if no deadlines are missed in this schedule. The schedulability analysis has a pseudo-polynomial complexity of $O(N \sum_{i=1}^{N} \frac{\min\{\tau,\Omega\}}{h_i})$ [44]). If such a feasible schedule exists, $\beta_{opt} = \beta$ (Line 6). Otherwise, β is set to $\frac{\beta_{up}+\beta_{low}}{2}$ (Line 9). In each iteration of the algorithm, the optimization problem (29) with the current β value is solved to determine the optimal delay values for all $i \in [1, N]$ (Line 10). Then, the feasibility of constructing a schedule with the optimal delay and period

Algorithm 1 Energy Minimizing Schedule Generation Algorithm (EMSA)

1: $\beta_{suf} = \min\{1, \min_{i\in[1,N]} \frac{\Delta}{h_i^*}\}$; $\beta_{nec} = 1$;
2: $\beta_{low} = \beta_{suf}$; $\beta_{up} = \beta_{nec}$;
3: $\beta = \beta_{up}$;
4: $\{d_i^*, i \in [1, N]\}$ = **solveOptim**(β);
5: **if isSchedulable**($\{h_i^*, d_i^*, i \in [1, N]\}$) **then**
6: $\quad\beta_{opt} = \beta$;
7: **else**
8: $\quad$**while** $\beta_{up} - \beta_{low} >= \epsilon$ **do**
9: $\quad\quad\beta = (\beta_{up} + \beta_{low})/2$;
10: $\quad\quad\{d_i^*, i \in [1, N]\}$ = **solveOptim**(β);
11: $\quad\quad$**if isSchedulable**($\{h_i^*, d_i^*, i \in [1, N]\}$) **then**
12: $\quad\quad\quad\beta_{low} = \beta$;
13: $\quad\quad$**else**
14: $\quad\quad\quad\beta_{up} = \beta$;
15: $\quad\quad$**end if**
16: $\quad$**end while**
17: $\quad\beta_{opt} = \beta_{low}$;
18: **end if**
19: $\{d_i^*, i \in [1, N]\}$ = **solveOptim**(β_{opt});
20: schedule = **EDFSchedule**($\{h_i^*, d_i^*, i \in [1, N]\}$);

values is checked (Line 11). If there exists a feasible schedule, β_{low} is set to β (Line 12); otherwise, β_{up} is set to β (Line 14). β is then updated with the value $\frac{\beta_{up}+\beta_{low}}{2}$ (Line 9). The algorithm stops when β_{low} and β_{up} get sufficiently close to each other such that $\beta_{up} - \beta_{low} < \epsilon$ (Line 8) where ϵ is a predetermined arbitrarily small constant. β_{opt} is then set to β_{low} (Line 17). Finally, the joint optimization problem (29) is solved for $\beta = \beta_{opt}$ (Line 19). The corresponding feasible schedule is constructed by the EDF scheduling algorithm over one scheduling frame (Line 20, **EDFSchedule**($\{h_i, d_i, i \in [1, N]\}$) function constructs the EDF schedule corresponding to the given period and delay values over one scheduling frame. The function first generates the EDF schedule over the time duration of length Ω and then repeats the schedule n_{MATI} times since the length of the scheduling frame is equal to $n_{MATI}\Omega$).

EMSA algorithm requires at most $K = \lceil \log_2[(\beta_{nec} - \beta_{suf})/\epsilon] \rceil$ exact schedulability analyses performed by **isSchedulable**($\{h_i, d_i, i \in [1, N]\}$) function since the value of $(\beta_{nec} - \beta_{suf})$ is decreased by half at each iteration until it becomes less than ϵ and one EDF schedule construction performed by **EDFSchedule**($\{h_i, d_i, i \in [1, N]\}$). For example, for an ϵ value of 0.001, the maximum number of exact schedulability analyses in EMSA is $K = 10$ since the maximum value of $(\beta_{nec} - \beta_{suf})$ is equal to 1.

V. Performance Evaluation

The goal of this section is to evaluate the energy saving of the proposed joint optimization problem over the traditional separate design of controller and communication systems. In the traditional separate design of these systems, which is denoted by "TS", the constellation size and sampling period of the sensor nodes are predetermined. For instance, WirelessHart [9] and ISA100.11a [8], which are the two competing wireless standards for industrial control applications, employ O-QPSK (Offset Quadrature Phase Shift Keying) without optimizing the constellation size nor the sampling period. In "TS", the values of the fixed constellation size and sampling period of the sensor nodes are determined such that the existence of a solution is guaranteed for the worst case scenario with no adjustment to different network and channel conditions. For instance, when we analyze the variability of the energy consumption as a function of MAD, we choose one of the constellation size values that is feasible for all MAD values. The proposed heuristic algorithm for the joint optimization of these systems, which is denoted by "HS", follows the procedure described in Section IV-A to determine the optimal parameters including $b_i^{\min}$, $k_i^*(b_i) = k_i(b_i^{\min})$, $b_i^{\max}$, h_i^* and q_i^* for each $i \in [1, N]$ separately and the optimal constellation size b_i^* for all $i \in [1, N]$ by solving the relaxation of the IP problem (29) with the optimal utilization bound β_{opt} and ceiling the non-integral solution values to obtain a feasible integral solution. To understand the maximum deviation of the HS algorithm from the optimal formulation, we have also included the optimal solution, denoted by "OPT". This optimal solution is obtained by exhaustive search where every feasible solution of the IP problem (29) with $\beta = 1$ that yields a feasible EDF schedule is enumerated and the one with the minimum power consumption is determined. This exhaustive search has exponential computational complexity in the network size.

TABLE I
Simulation Parameters

σ^2	-174 dBm/Hz	B	10 KHz
$W^{t,\max}$	250 mW	W^c	50mW
$L_i, i \in [1, N]$	100 bits	δ	0.95
N^f	10 dB	G^c	1 (uncoded) [27]

Simulation results are obtained based on 1000 independent random network topologies where the sensor nodes are uniformly distributed within a circular area of radius r transmitting to a controller located in the center of the area. The parameters used in the simulations are given in Table-I.

The attenuation of the links are determined considering both large scale statistics that arise primarily from the free space loss and the environment affecting the degree of refraction, diffraction, reflection and absorption, and small scale statistics that occur due to multipath propagation and variations in the environment. The dependence of the path loss on distance summarizing large scale statistics is modeled as

$$PL(d) = PL(d_0) + 10\alpha \log(d/d_0) + Z \tag{31}$$

where d is the distance between the transmitter and receiver, $PL(d)$ is the path loss at distance d in decibels, $PL(d_0) = 70$ dB is the path loss at reference distance $d_0 = 1$ m, $\alpha = 3.5$ is the path loss exponent [27] and Z is a Gaussian random variable with zero mean and standard deviation equal to 4 dB [47]. The small-scale fading on the other hand has been modeled by using Nakagami fading with scale parameter Ω set to the mean power level determined by using Eq. (31) and shape parameter m chosen from the set $\{1, 3, 5\}$ [47], [48]. Note that Nakagami fading with shape parameter equal to 1 corresponds to Rayleigh fading. In the first part of the simulations including Figs. 3- 7, the channel is assumed fixed at the mean value determined based on the large scale statistics. In the second part of the simulations including Figs. 8- 10, the robustness of the proposed algorithm to the time-varying channel conditions is analyzed by considering small-scale statistics.

Fig. 3 shows the average power consumption in a network of 20 nodes at different average distances from the controller. The average distance is calculated by taking the average of the distances of the nodes randomly distributed within a circle of different radii. The MAD and MATI values are chosen as $\Delta = 5$ ms and $\Omega = 100$ ms. The effect of the average distance on the average power consumption is twofold. First, as the distance increases, the transmit power required to compensate for the increasing attenuation increases. Since the power consumption is proportional to the transmit power, increasing the transmit power also increases the power consumption. Second, as the distance increases, the maximum feasible constellation size imposed by the maximum transmit power constraint decreases shrinking the feasible region over which the power consumption is minimized. This accelerates the increase in the power consumption by increasing distance. The constellation size for the TS algorithm is determined such that it is feasible for the maximum distance value since feasibility for maximum distance guarantees feasibility for

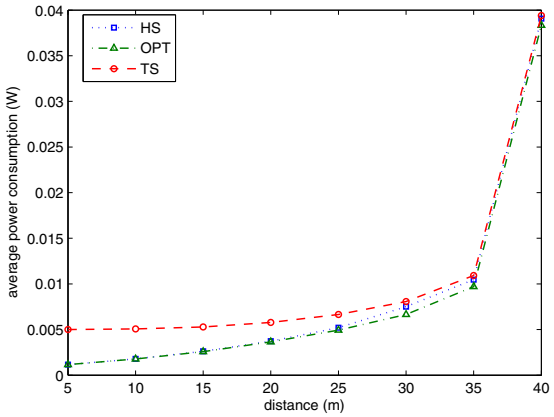

Fig. 3. Average power consumption in a network of 20 nodes at different average distances from the controller where $\Delta = 5$ ms and $\Omega = 100$ ms.

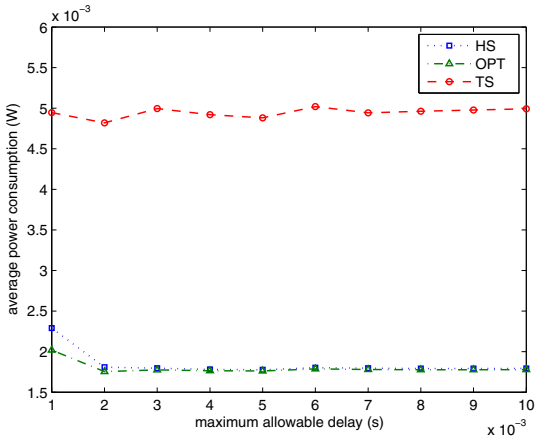

Fig. 4. Average power consumption in a network of 20 nodes for different MAD values where nodes are uniformly distributed within a circular area of radius 10 m and $\Omega = 200$ ms.

lower distance values. Hence, the HS algorithm outperforms the TS algorithm significantly for relatively small average distance values. Moreover, the HS algorithm performs very close to the OPT independent of the distance value, by an approximation ratio of around 1.01 where approximation ratio is defined as the ratio of the solution of the HS algorithm to the optimal solution.

Fig. 4 shows the average power consumption in a network of 20 nodes for different MAD values. The nodes are uniformly distributed within a circular area of radius 10 m and the MATI value is chosen as $\Omega = 200$ ms. The MAD constraint determines the minimum constellation size together with $\Omega/k_i(b_i^{\min})$ as explained in detail in Section IV-A. As the MAD increases up to a certain value, around 2 ms, the average power consumption decreases since for smaller MAD values, the nodes in the network are forced to choose greater constellation size values, which increases the power consumption dramatically. On the other hand, as the MAD increases further, the average power consumption stays constant due to the fact that the optimal constellation size remains constant although the feasible region expands. The constellation size for the TS algorithm is determined such that it is feasible for the minimum MAD value since then feasibility of all MAD values is ensured. Since the power consumption function does not depend on the MAD value, the resulting power consumption of the TS algorithm remains constant for different MAD values and is dramatically worse than the HS algorithm which performs very close to the OPT, by an average approximation ratio of around 1.02.

Fig. 5 shows the average power consumption in a network of 20 nodes for different MATI values. The nodes are uniformly distributed within a circular area of radius 10 m and the MAD value is chosen as $\Delta = 10$ ms. Since the power consumption is a decreasing function of MATI, the average power consumption decreases as the MATI increases. However, the effect of the MATI on the average power consumption in a network is not limited to this functional dependency for the HS algorithm. The schedulability constraint given by Eq. (29b) suggests that for small MATI values, the objective of power minimization requires a joint decision among multiple nodes in the network since minimizing the power consumption independently for each node in the network may result in the violation of the schedulability constraint. Hence, as the MATI decreases, the amount of increase in the power consumption is much more than the functional dependency of the power consumption on the MATI. For example, when we increase the MATI from 15 ms to 20 ms, the power consumption is expected to decrease by 33% but actually decreases by 50%. On the other hand, for the TS algorithm, the effect of the MATI on the power consumption is limited to the functional dependency of the power consumption on the MATI. Again, the HS algorithm performs very close to the OPT, by an approximation ratio of around 1.05, and outperforms the TS algorithm which has an approximation ratio of more than 2 for large MATI values. The performance of the TS algorithm is relatively better for smaller MATI values since the predetermined constellation size value is adjusted considering the feasibility for the minimum MATI value but still much worse than the performance of the HS algorithm.

Fig. 6 shows the average power consumption for different number of nodes. The nodes are uniformly distributed within a circular area of radius 5 m. The MAD and MATI values are chosen as $\Delta = 25$ ms and $\Omega = 25$ ms. For the HS algorithm, as the number of nodes increases up to a specific value, i.e. 25 in this case, depending on the MATI, the power consumption increases linearly since the objective of the power minimization does not require a joint decision among multiple nodes in the network meaning that minimizing the power consumption independently for each node does not result in the violation of the schedulability constraint. However, as the number of nodes increases further, a joint decision is necessary to satisfy the schedulability constraint. The nodes in the network are forced to choose higher constellation size than they would choose when they minimize their power consumption independently. This causes a much faster increase in the power consumption. The average approximation ratio of the HS algorithm is 1.03. The resulting power consumption of the TS algorithm on the other hand increases linearly as expected since the

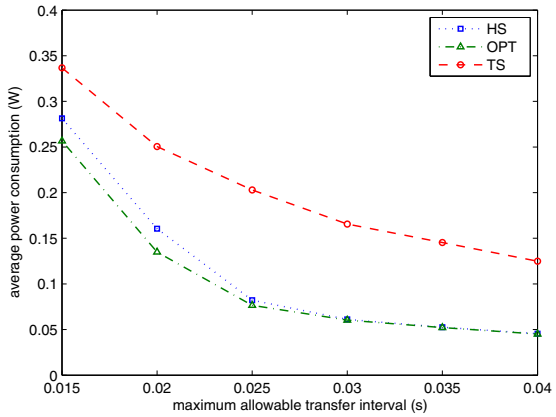

Fig. 5. Average power consumption in a network of 20 nodes for different MATI values where nodes are uniformly distributed within a circular area of radius 10 m and $\Delta = 10$ ms.

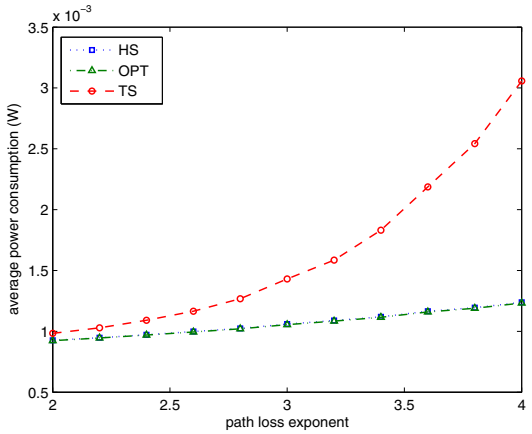

Fig. 7. Average power consumption for different path loss exponent values in a network of 20 nodes where nodes are uniformly distributed within a circular area of radius 5 m, $\Delta = 10$ ms and $\Omega = 100$ ms.

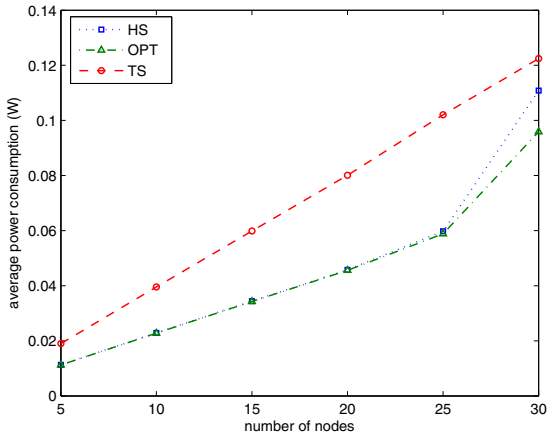

Fig. 6. Average power consumption for different number of nodes where nodes are uniformly distributed within a circular area of radius 5 m, $\Delta = 25$ ms and $\Omega = 25$ ms.

predetermined constellation size is constant. The performance of the TS algorithm is much worse than that of the HS algorithm with an average approximation ratio of 1.65.

Fig. 7 shows the average power consumption in a network of 20 nodes for different path loss exponent values. The nodes are uniformly distributed within a circular area of radius 5 m. The MAD and MATI values are chosen as $\Delta = 10$ ms and $\Omega = 100$ ms. The constellation size of the TS algorithm is determined such that it is feasible for the highest path loss exponent and highest distance from the controller since then feasibility for all path loss exponent values and all the nodes in the network is guaranteed. For fixed values of the constellation size and remaining communication parameters used in the TS algorithm, the power consumption increases exponentially with the path loss exponent. The reason for this exponential increase is that the transmit power required to compensate for the increasing attenuation in an environment of larger path loss exponent increases exponentially based on the path loss model given in Eq. (31) and the power consumption is proportional to the transmit power. The average power consumption of the HS algorithm on the other hand increases linearly with the path loss exponent since the constellation size is optimized at every node in the network for all the path loss exponent values. The average approximation ratio of the HS algorithm is 1.01. The difference between TS and HS algorithms increases as the path loss exponent increases since higher path loss exponent creates more variation of the optimal constellation size of the nodes in the network increasing the value of optimizing the communication parameters of the sensor nodes in the network.

Figs. 8, 9 and 10 show the robustness of the proposed algorithm over time by considering the time-varying channel condition modeled using Rayleigh fading, Nakagami fading with shape parameter $m = 3$ and $m = 5$ respectively. We assume that the fading level is available to the transmitter through a causal Channel State Information (CSI) feedback at the beginning of each transmission interval. As the distance of the node from the controller and fading level increases, the maximum feasible constellation size imposed by the maximum transmit power constraint decreases shrinking the feasible region over which the power consumption is minimized. Therefore, the constellation size of the TS algorithm is chosen as the minimum value in the feasibility region. Similar to the analysis of the effect of the path loss exponent on the power consumption, the power consumption of the TS algorithm employing fixed constellation over all fading levels increases significantly when the fading level is high. The reason for this increase is that the transmit power required to compensate for the increasing attenuation increases and the power consumption is proportional to the transmit power. This also causes large fluctuations in the power consumption of the TS algorithm over time. The amount of these fluctuations on the other hand depends on the variance of the fading distribution. The fluctuations increases when the fading distribution changes from Nakagami fading with $m = 5$ to Nakagami fading with $m = 3$ and from Nakagami fading with $m = 3$ to Rayleigh fading. Furthermore, the average power consumption of the HS algorithm is stable over time and very close to the

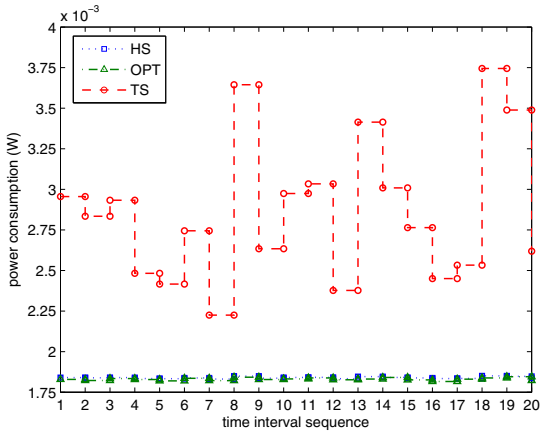

Fig. 8. Power consumption in a network of 20 nodes under Rayleigh fading where nodes are uniformly distributed within a circular area of radius 5 m, $\Delta = 10$ ms and $\Omega = 100$ ms.

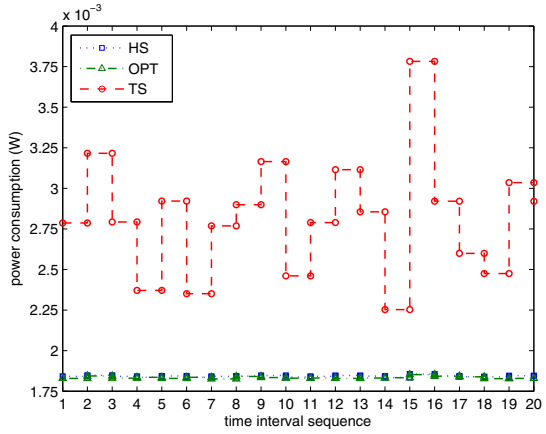

Fig. 9. Power consumption in a network of 20 nodes under Nakagami fading with $m = 3$ where nodes are uniformly distributed within a circular area of radius 5 m, $\Delta = 10$ ms and $\Omega = 100$ ms.

optimal with average approximation ratio less than 1.01 for all three fading distributions since the values of the parameters are optimized according to the channel information at the beginning of each interval.

VI. Conclusion

A joint design of communication and control application layers is studied by considering a constrained optimization problem, for which the objective function is the power consumption of the network and the constraints are the reliability and delay requirements for the stability of the control systems and the schedulability and maximum transmit power constraints of the communication systems. The decision variables of this optimization problem are the sampling period of the control layer, the constellation size of the modulation and the probability of error of the communication layer. The optimization problem is first formulated as a Mixed-Integer Programming problem. Upon deriving the relation of the optimal sampling period and packet error probability to the optimal constellation size, the problem is reduced to an IP problem. We propose an efficient solution method based on the relaxation of this IP problem. Extensive simulation results show that the performance of the proposed solution procedure is very close to the optimal solution and much better than the traditional separate design of controller and communication systems for varying network and control system parameters and under different fading channel models.

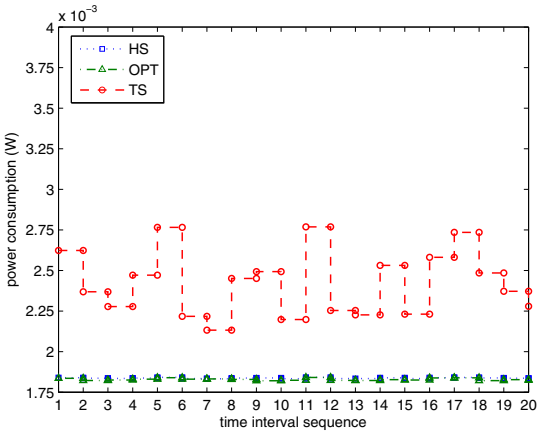

Fig. 10. Power consumption in a network of 20 nodes under Nakagami fading with $m = 5$ where nodes are uniformly distributed within a circular area of radius 5 m, $\Delta = 10$ ms and $\Omega = 100$ ms.

References

[1] J. P. Hespanha, P. Naghshtabrizi, and Y. Xu, "A survey of recent results in networked control systems," *Proc. IEEE*, vol. 95, no. 1, pp. 138–162, Jan. 2007.

[2] A. Willig, "Recent and emerging topics in wireless industrial communication," *IEEE Trans. Industrial Inf.*, vol. 4, no. 2, pp. 102–124, May 2008.

[3] J. R. Moyne and D. M. Tilbury, "The emergence of industrial control networks for manufacturing control, diagnostics, and safety data," *Proc. IEEE*, vol. 95, no. 1, pp. 29–47, Jan. 2007.

[4] A. Aswani, N. Master, J. Taneja, D. Culler, and C. Tomlin, "Reducing transient and steady state electricity consumption in HVAC using learning-based model-predictive control," *Proc. IEEE*, vol. 100, no. 1, pp. 240–253, Jan. 2012.

[5] P. Varaiya, "Smart cars on smart roads: problems of control," *IEEE Trans. Automatic Control*, vol. 38, no. 2, pp. 195–207, Feb. 1993.

[6] Minimum Aviation System Performance Standard for Automatic Dependent Surveillance Broadcast (ADS-B), RTCA, 2002, DO-242A.

[7] H. Li, L. Lai, and H. V. Poor, "Multicast routing for decentralized control of cyber physical systems with an application in smart grid," *IEEE J. Sel. Areas Commun.*, vol. 30, no. 6, pp. 1097–1107, July 2012.

[8] ISA-100.11a-2009 Wireless systems for industrial automation: Process control and related applications, ISA, 2009.

[9] Wirelesshart data sheet, HART Communication Foundation, 2007. Available: http://www.hartcomm2.org/hartprotocol/wirelesshart/wirelesshartmain.html.

[10] R. Steigman, and J. Endresen, "Introduction to WISA and WPS, WISA-wireless interface for sensors and actuators and WPS-wireless proximity switches," white paper, 2004. Available: http://www.eit.uni-kl.de/litz/WISA.pdf.

[11] R. A. Gupta and M. Chow, "Networked control system: overview and research trends," *IEEE Trans. Industrial Electron.*, vol. 57, no. 7, pp. 2527–2535, July 2010.

[12] N. Pereira, B. Andersson, and E. Tovar, "Widom: a dominance protocol for wireless medium access," *IEEE Trans. Industrial Inf.*, vol. 3, no. 2, pp. 120–130, May 2007.

[13] H. Hoang, G. Buttazzo, M. Jonsson, and S. Karlsson, "Computing the minimum EDF feasible deadline in periodic systems," in *Proc. 2006 IEEE Real-Time Syst. Symp.*, pp. 125–134.

[14] Y. Wu, G. Buttazzo, E. Bini, and A. Cervin, "Parameter selection for real-time controllers in resource-constrained systems," *IEEE Trans. Industrial Inf.*, vol. 6, no. 4, pp. 610–620, Nov. 2010.
[15] M. Baldi, R. Giacomelli, and G. Marchetto, "Time-driven access and forwarding for industrial wireless multihop networks," *IEEE Trans. Industrial Inf.*, vol. 5, no. 2, pp. 99–112, May 2009.
[16] B. Demirel, Z. Zou, P. Soldati, and M. Johansson, "Modular co-design of controllers and transmission schedules in wirelesshart," in *Proc. 2011 IEEE Conf. Decision Control European Control*, pp. 5951–5958.
[17] P. Park, J. Araujo, and K. H. Johansson, "Wireless networked control system co-design," in *Proc. 2011 IEEE International Conf. Netw., Sensing and Control*, pp. 486–491.
[18] J. Bai, E. P. Eyisi, F. Qiu, Y. Xue, and X. D. Koutsoukos, "Optimal cross-layer design of sampling rate adaptation and network scheduling for wireless networked control systems," in *Proc. 2012 ACM/IEEE International Conf. Cyber-Physical Syst.*, pp. 107–116.
[19] X. Liu and A. Goldsmith, "Wireless network design for distributed control," in *Proc. 2004 IEEE Conf. Decision Control*, pp. 2823–2829.
[20] E. Uysal-Biyikoglu, B. Prabhakar, and A. E. Gamal, "Energy-efficient packet transmission over a wireless link," *IEEE/ACM Trans. Netw.*, vol. 10, no. 4, pp. 487–499, Aug. 2002.
[21] A. Fu, E. Modiano, and J. N. Tsitsiklis, "Optimal transmission scheduling over a fading channel with energy and deadline constraints," *IEEE Trans. Wireless Commun.*, vol. 5, no. 3, pp. 630–641, Mar. 2006.
[22] M. A. Antepli, E. Uysal-Biyikoglu, and H. Erkan, "Optimal packet scheduling on an energy harvesting broadcast link," *IEEE J. Sel. Areas Commun.*, vol. 29, no. 8, pp. 1721–1731, Sept. 2011.
[23] O. Ozel, J. Yang, and S. Ulukus, "Optimal broadcast scheduling for an energy harvesting rechargeable transmitter with a finite capacity battery," *IEEE Trans. Wireless Commun.*, vol. 11, no. 6, pp. 2193–2203, June 2012.
[24] W. Chen, M. J. Neely, and U. Mitra, "Energy-efficient transmissions with individual packet delay constraints," *IEEE Trans. Inf. Theory*, vol. 54, no. 5, pp. 2090–2109, May 2008.
[25] X. Zhong and C. Wu, "Energy-efficient wireless packet scheduling with quality of service control," *IEEE Trans. Mobile Comput.*, vol. 6, no. 10, pp. 1158–1170, Oct. 2007.
[26] M. A. Zafer and E. Modiano, "A calculus approach to energy-efficient data transmission with quality-of-service constraints," *IEEE/ACM Trans. Netw.*, vol. 17, no. 3, pp. 898–911, June 2009.
[27] S. Cui, A. J. Goldsmith, and A. Bahai, "Energy-constrained modulation optimization," *IEEE Trans. Wireless Commun.*, vol. 4, no. 5, pp. 2349–2360, Sept. 2005.
[28] T. Arampatzis, J. Lygeros, and S. Manesis, "A survey of applications of wireless sensors and wireless sensor networks," in *Proc. 2005 IEEE International Symp. Mediterrean Conf. Control Automation*, pp. 719–724.
[29] S. Ergen and P. Varaiya, "Pedamacs: power efficient and delay aware medium access protocol for sensor networks," *IEEE Trans. Mobile Comput.*, vol. 5, no. 7, pp. 920–930, June 2006.
[30] G. Walsh, O. Beldiman, and L. Bushnell, "Asymptotic behavior of nonlinear networked control systems," *IEEE Trans. Automatic Control*, vol. 46, no. 7, pp. 1093–1097, July 2001.
[31] G. Walsh, H. Ye, and L. Bushnell, "Stability analysis of networked control systems," *IEEE Trans. Control Syst. Technol.*, vol. 10, no. 3, pp. 438–446, May 2002.
[32] D. Carnevale, A. R. Teel, and D. Nesic, "A Lyapunov proof of an improved maximum allowable transfer interval for networked control systems," *IEEE Trans. Automatic Control*, vol. 52, no. 5, pp. 892–897, May 2007.
[33] W. P. M. H. Heemels, A. R. Teel, N. van de Wouw, and D. Nesic, "Networked control systems with communication constraints: tradeoffs between transmission intervals, delays and performance," *IEEE Trans. Automatic Control*, vol. 55, no. 8, pp. 1781–1796, Aug. 2010.
[34] G. Karagiannis, O. Altintas, E. Ekici, G. Heijenk, B. Jarupan, K. Lin, and T. Weil, "Vehicular networking: a survey and tutorial on requirements, architectures, challenges, standards and solutions," *IEEE Commun. Surveys Tuts.*, vol. 13, no. 4, pp. 584–616, July 2011.
[35] *Industrial communication networks - Wireless communication network and communication profiles - WirelessHART*, IEC, iEC 62591.
[36] IEEE 802.15.4 standard: Wireless Medium Access Control and Physical Layer Specifications for Low-Rate Wireless Personal Area Networks, IEEE, 2006. Available: http://www.ieee802.org/15/pub/TG4.html.
[37] IEEE 802.15 task group 4e: Wireless Medium Access Control and Physical Layer Specifications for Low-Rate Wireless Personal Area Networks, IEEE, 2012. Available: http://www.ieee802.org/15/pub/TG4e.html.
[38] P. Park, C. Fischione, A. Bonivento, K. Johansson, and A. Sangiovanni-Vincent, "Breath: an adaptive protocol for industrial control applications using wireless sensor networks," *IEEE Trans. Mobile Comput.*, vol. 10, no. 6, pp. 821–838, June 2011.
[39] T. M. Cover and J. A. Thomas, *Elements of Information Theory*. Wiley-Interscience, 1991.
[40] J. Proakis, *Digital Communications*. McGraw-Hill, 2000.
[41] M. I. of Technology, Project MAC. Engineering Robotics Group and M. Dertouzos, *Control robotics: The procedural control of physical processes*, 1973.
[42] S. Baruah and J. Goossens, "Scheduling real-time tasks: algorithms and complexity," *Handbook of Scheduling: Algorithms, Models, and Performance Analysis*, vol. 3, 2004.
[43] F. Eisenbrand and T. Rothvoß, "EDF-schedulability of synchronous periodic task systems is conp-hard," in *Proc. 2010 ACM-SIAM Symp. Discrete Algorithms*, pp. 1029–1034.
[44] F. Zhang and A. Burns, "Schedulability analysis for real-time systems with EDF scheduling," *IEEE Trans. Comput.*, vol. 58, no. 9, pp. 1250–1258, Sept. 2009.
[45] S. Boyd and L. Vandenberghe, *Convex Optimization*. Cambridge University Press, 2004.
[46] D. Bertsimas and T. Tsitsiklis, *Introduction to Linear Optimization*. Athena Scientific, 1997.
[47] O. Khader, A. Willig, and A. Wolisz, "A simulation model for the performance evaluation of wirelesshart TDMA protocol," technical report, Telecommunication Networks Group, Technical UniversityBerlin, TKN Technical Report Series TKN-11-001, Berlin, Germany, Tech. Rep., 2011.
[48] A. F. Molisch, K. Balakrishnan, C.-C. Chong, S. Emami, A. Fort, J. Karedal, J. Kunisch, H. Schantz, U. Schuster, and K. Siwiak, "IEEE 802.15. 4a channel model-final report," *IEEE P802*, vol. 15, no. 04, p. 0662, 2004.

Yalcin Sadi received the B.S. and M.S. degrees in electrical and electronics engineering from Koc University in 2010 and 2012. He is currently a Ph.D. student in electrical and electronics engineering in Koc University and working in Wireless Networks Laboratory under supervision of Prof. Sinem Coleri Ergen. His research interests are communication design in wireless networks and intra-vehicular wireless sensor networks. He received Tubitak (The Scientific and Technological Research Council of Turkey) Fellowship in 2010 and Koc University Full Merit Scholarship from Koc University in 2005.

Sinem Coleri Ergen received the BS degree in electrical and electronics engineering from Bilkent University in 2000, the M.S. and Ph.D. degrees in electrical engineering and computer sciences from University of California Berkeley in 2002 and 2005. She worked as a research scientist in Wireless Sensor Networks Berkeley Lab under sponsorship of Pirelli and Telecom Italia from 2006 to 2009. Since September 2009, she has been Assistant Professor in the department of Electrical and Electronics Engineering at Koc University. Her research interests are in wireless communications and networking with applications in sensor networks and transportation systems. She received Turk Telekom Collaborative Research Award in 2011 and 2012, Marie Curie Reintegration Grant in 2010, Regents Fellowship from University of California Berkeley in 2000 and Bilkent University Full Scholarship from Bilkent University in 1995.

Pangun Park received the M.S. and Ph.D. degrees in electrical engineering from the Royal Institute of Technology, Sweden, in 2007 and 2011, respectively. He worked as a postdoctoral researcher at the University of California at Berkeley, CA from 2011 to 2013. Since 2013, he has been working as a senior researcher in Electronics and Telecommunications Research Institute, South Korea. He received the best paper award at the IEEE International Conference on Mobile Ad-hoc and Sensor System of 2009. His research interests include cyber-physical systems, networked control systems, and wireless sensor and actuator networks.